Morphine reprograms brain-derived extracellular vesicles from cargo linked to synaptic remodelling in the prefrontal cortex

Pedro Henrique Gobira[1]; Savio Bastos[1]; Rachele Rossi [2]; Christian Bjerggaard Vægter[2]; Fenghua Chen[1]; Nicole Rodrigues da Silva[2]; Heidi Kaastrup Müller[1], Samia Joca[2]; Thomas Boesen [3]; Thiago Wendt Viola [4]; Yan Yan [5]; Martin R. Larsen[6]; Victor Corasolla Carregari [6]; Rodrigo Grassi-Oliveira*[1,4]

[1] Translational Neuropsychiatry Unit, Department of Clinical Medicine, Aarhus University, Aarhus, Denmark; [2] Aarhus University, Biomedicine, Aarhus, Denmark; [3] Interdisciplinary Nanoscience Center -iNANO, Aarhus University, Aarhus; [4] Nanopsychiatry Lab, School of Medicine, Pontifical Catholic University of Rio Grande do Sul (PUCRS), Brazil; [5] EVGenomics ApS, Aarhus, Denmark; [6] Department of Biochemistry and Molecular Biology, University of Southern Denmark, Odense, Denmark.

* Correspondence: Rodrigo Grassi-Oliveira. Palle Juul-Jensens Boulevard 11 8200 Aarhus N Denmark rogo@clin.au.dk, rodrigo.grassi@pucrs.br

Abstract

Extracellular vesicles (EVs) released by neurons and glial cells mediate intercellular communication in the brain and regulate synaptic function, neuronal survival, and neuropathological processes. Although chronic opioid exposure induces widespread neuroadaptations, the contribution of brain-derived EVs (BDEVs) to these processes remains largely unknown. Here, we isolated BDEVs from the prefrontal cortex of rats chronically exposed to morphine and performed integrative transcriptomic and proteomic analyses of their molecular cargo. Total RNA sequencing combined with unbiased proteomics revealed that morphine profoundly reprograms the BDEV transcriptome and proteome, enriching pathways related to synaptic plasticity, endoplasmic reticulum (ER) stress, mitochondrial dysfunction, and neurodegeneration. Among the most prominent alterations, the synaptic regulator *ARC* was consistently modulated at the mRNA level, while the ER stress marker *HSPA5* was altered at both mRNA and protein levels. Functional assays further demonstrated that BDEVs derived from morphine-treated rats were sufficient to reconfigure transcriptional programs in naïve cortical neurons, affecting genes associated with synaptic remodeling and excitability. Collectively, these findings provide the first evidence that chronic opioid exposure reprograms BDEV cargo in a brain region critical for addiction and that these vesicles can propagate transcriptional reorganization to recipient neurons. BDEVs thus emerge as active mediators of morphine-induced neuroadaptations and as potential targets for biomarker discovery and therapeutic intervention in opioid use disorder.

extracellular vesicles; morphine; prefrontal cortex; transcriptomics; proteomics; synaptic plasticity

Introduction

Opioid use disorder (OUD) remains a major public health crisis, driven by persistent neuroadaptations that underlie compulsive drug seeking and relapse [1,2]. Although the synaptic and receptor-level effects of opioids have been extensively characterized [3,4] , the intercellular mechanisms through which prolonged exposure remodels brain circuits are still not fully understood. Bridging this gap requires examining how cells communicate beyond classical synaptic signaling, through molecular messengers capable of propagating neuroadaptations across neural networks.

Extracellular vesicles (EVs) are nanosized particles secreted by virtually all cell types, including neurons and glia, that transport proteins, RNAs, and lipids between cells [5]. Within the central nervous system, brain-derived EVs (BDEVs) regulate synaptic plasticity, stress responses, and neuronal survival [6-8]. Given their ability to mediate intercellular communication, BDEVs have emerged as key candidates for understanding how chronic drug exposure reshapes brain function. Disruptions in these processes have been increasingly implicated in psychiatric conditions, including substance use disorders [8]. However, although emerging evidence suggests that drugs of abuse can modify the molecular cargo of EVs, the link between such changes and broader neurobiological processes remains poorly defined [9].

Most prior work has focused on small RNAs, particularly microRNAs, based on the assumption that EVs are selectively enriched for these species [10,11]. Yet this focus may overlook critical layers of regulation, as recent studies demonstrate that BDEVs can also deliver intact mRNAs, such as the synaptic regulator ARC, which are translated in recipient neurons and contribute to neuroadaptive remodelling across interconnected brain regions [12,13]. These findings suggest that EVs may act as functional conveyors of complex molecular programs, extending opioid-induced neuroplasticity beyond synaptic boundaries.

Here, we test the hypothesis that chronic morphine exposure reprograms the transcriptomic and proteomic composition of BDEVs and that these vesicles are sufficient to drive transcriptional changes in recipient neurons. We isolated BDEVs from the prefrontal

cortex (PFC), a region central to addiction-related plasticity, and conducted integrative RNA sequencing and proteomic profiling. Functional validation was performed by exposing primary cortical neurons to BDEVs derived from morphine- or vehicle-treated rats, followed by transcriptional analyses. Together, these experiments identify BDEVs as potential mediators of opioid-induced neuroadaptations, providing novel insights into the pathophysiology of OUD and highlighting opportunities for biomarker development and therapeutic innovation.

Methods and Materials

Methods are summarized below. A complete description of all experimental procedures is available in Supplementary Materials.

Animals and drug treatment

Male Sprague–Dawley rats (8 weeks old, Janvier Labs) were pair-housed under standard conditions with ad libitum access to food and water. After two weeks of habituation, animals received intraperitoneal injections of saline or escalating doses of morphine (10–50 mg/kg, twice daily for 5 days). Four hours after the final injection, rats were sacrificed, and bilateral PFC was dissected and frozen at −80 °C. All procedures were approved by the Danish Animal Experiments Inspectorate and complied with EU Directive 2010/63/EU.

Isolation and characterization of brain-derived extracellular vesicles (BDEVs)

BDEVs were isolated from PFC tissue by enzymatic dissociation, differential centrifugation, filtration, and ultracentrifugation, as previously described [14]. Vesicle purity and morphology were assessed by BCA protein assay, Western blotting, transmission electron microscopy (TEM), and nanoparticle tracking analysis (NTA). Full protocols are provided in Supplementary Methods.

RNA extraction, sequencing, and analysis

RNA was extracted from BDEVs, DNA was removed, and total RNA libraries were prepared using a stranded RNA-seq kit. Libraries were sequenced on an Illumina NovaSeq X Plus platform (150 bp, paired-end). Quality control, differential gene expression analysis (DESeq2), and pathway enrichment (Metascape, GO, and Reactome) followed standard procedures, with significance defined at FDR-adjusted $p < 0.1$ and log2FC ±0.5.

Proteomic analysis

BDEV proteins were extracted, digested with trypsin, and analyzed by LC–MS/MS on an Orbitrap Q Exactive HF system. Data were searched against the Rattus norvegicus UniProt database and filtered at 1% FDR. Proteins were quantified based on unique peptides, and enrichment analyses were conducted using Cytoscape, IPA, and R-based workflows.

Primary neuronal cultures and BDEV treatment

Cortical neurons were prepared from embryonic day 17 (E17) C57BL/6 embryos and plated in Neurobasal medium with B27 supplement. On DIV7, neurons were treated with BDEVs isolated from saline- or morphine-exposed rats, and RNA was extracted 24 h later.

NanoString gene expression profiling

Gene expression in primary neurons was measured using the NanoString nCounter® Mouse Neuropathology Panel (770 genes). Data were normalized to housekeeping genes using nSolver™ 4.0, and pathway enrichment was conducted in Reactome.

Results

Characterization of EVs from the prefrontal cortex of chronically morphine-treated rats

BDEVs were isolated from the PFC of rats via ultracentrifugation as previously described [14]. We used NTA to determine the size distribution and particle number, with the latter normalized to the individual PFC weight. Results revealed no significant differences between animals treated with morphine and those treated with vehicle **(Fig. 1B).** Using TEM, we characterized the BDEVs, revealing their characteristic morphology (**Fig. 1C**). We also analyzed BDEVs via specific positive and negative markers via Western blotting. As expected, the positive markers flotillin-1 and Hsp70 were detected in the BDEV fractions, whereas the negative marker GM130 was absent from the BDEV fractions but present in the whole cortex lysates (**Fig. 1D**). Together, these findings confirm the reliability of our isolation technique.

Effect of morphine treatment on the RNA profile of BDEVs

The RNA-seq analysis identified a total of 12,224 RNA molecules that surpassed the quality control threshold for downstream analysis, comprising 49 long noncoding RNAs

(0.40%), 94 small noncoding RNAs (0.77%), 11,948 protein-coding mRNA molecules (97.74%), and other RNAs (e.g., ribosomal RNA, transfer RNA, mitochondrial RNA, and pseudogenes—1.09%). Prior to conducting the differential gene expression (DGE) analysis, the RNA-seq data were deconvoluted from publicly available single-cell RNA sequencing data from rodent brains. We analyzed the proportions of microglia, glutamatergic corticothalamic (CT), intratelencephalic (IT), and pyramidal tract (PT) neurons, as well as GABAergic interneurons. The proportions of oligodendrocytes, astrocytes, and glutamatergic NP neurons were negligible. No significant group differences in cell-type proportions were observed (all p values > 0.05; see **Fig.** 2A). However, we observed that almost 40% of the RNA-seq data were from BDEVs originating from GABAergic interneurons.

A comprehensive analysis revealed 625 RNA transcripts with unadjusted p values less than 0.05 (Supplemental Table 1), indicating an effect of morphine treatment on the EV transcriptomic cargo. Four hits were identified by DGE analysis as having significant group differences that surpassed the FDR correction thresholds: Arc, Hspa5, Hivep3, and RT1-CE16 **(Fig. 2B)**. These four molecules are mRNAs derived from protein-coding genes. Arc, Hspa5, and Hivep3 were upregulated in EVs from morphine-treated animals, whereas RT1-CE16 was downregulated. Additionally, we cross-referenced our RNA-seq data with a large-scale human genome-wide association study (GWAS) meta-analysis of opioid use disorder [15] to identify differentially regulated transcripts originating from previously identified genes associated with the disorder, such as Oprm1, Cdkal1, Btnl2, Rabepk, Fbxw4, Ncam1, Furin, Kcnn1, and Rnf114. Among these, two transcripts, Ncam1 (log2FC = 0.45; p value = 0.02) and Kcnn1 (log2FC = 0.49; p value = 0.04), had unadjusted p values below 0.05, indicating a greater abundance of EVs in morphine-treated animals than in control animals **(Fig. 2C).**

Pathway enrichment analysis was conducted using all RNAs with an unadjusted p value < 0.05 on the basis of the KEGG 2019 mouse database (*Rattus norvegicus* gene codes were converted to mice before enrichment). Among the enriched pathways, only Lysosome, Protein Processing in the Endoplasmic Reticulum, and Axon Guidance were significantly represented, predominantly comprising upregulated transcripts (Figure y1 a-b). Notably, the enriched RNAs within each pathway were mutually exclusive, with no individual RNA shared across multiple pathways. This suggests a limited overlap and low interpathway correlation among the transcriptional alterations observed (Figure y2a-b).

Effect of morphine treatment on the protein profile of BDEVs

A total of 1007 proteins were reliably quantified, 379 of which passed the quality control criteria for downstream analysis. Among these, 82 proteins were found to be dysregulated on the basis of unadjusted p values < 0.05 (Supplemental Table 2), including 44 downregulated and 38 upregulated proteins. However, none of these changes remained statistically significant after false discovery rate (FDR) correction. Consequently, we adopted a more permissive threshold, selecting proteins with unadjusted p values < 0.01 and an absolute log2-fold change (log2FC) ≥ 0.5 to highlight potentially relevant alterations, which is consistent with prior proteomic studies applying exploratory thresholds in complex biological models [16,17]. Using these criteria, ten proteins were identified as differentially regulated in BDEVs following morphine exposure (Fig. 3). Among these proteins, Krt33a, Fabp5, Krt72, Sprr1a, and Pkp1 were downregulated, whereas Stx1b, Ywhag, Grm8, Hspa5, and Pdia3 were upregulated.

A volcano plot was used to visualize the overall distribution of protein abundance changes, clearly highlighting the most significantly dysregulated proteins (p value < 0.05). Furthermore, dynamic range analysis revealed a broad spectrum of protein abundances, indicating that both low- and high-abundance proteins were successfully identified and quantified, an important aspect of exosome proteomics that enables the detection of diverse cargo molecules (Figure 3a-b) [18,19].

To elucidate the biological implications of these morphine-associated protein alterations, pathway enrichment analysis was performed via the KEGG Mouse 2019 database [20]. The dysregulated proteins were significantly associated with pathways involved in neurodegenerative diseases, oxidative phosphorylation, nonalcoholic fatty liver disease, the citrate (TCA) cycle, retrograde endocannabinoid signaling, thermogenesis, and protein processing in the endoplasmic reticulum (Figure 3 C).

Inspection of the dysregulation patterns revealed notable enrichment of mitochondrial proteins, particularly members of the NDUF family, as well as COX1 and COX7A2L (Figure 3 D-E), which play essential roles in oxidative phosphorylation and energy metabolism, mechanisms implicated in neuropsychiatric disorders [21-23]. Additionally, the upregulation of the GRM5-encoded metabotropic glutamate receptor in the exosomal cargo of morphine-exposed subjects suggests potential activation of the phosphatidylinositol–calcium second messenger signaling pathway, which is known to influence synaptic plasticity and drug-related neuroadaptation [24,25].

Integrative analysis of differentially regulated RNAs and proteins

Proteomic analysis identified 1,084 proteins, of which 1,007 were quantifiable. Notably, more than 85% overlapped with transcripts detected at the mRNA level, demonstrating substantial concordance between the transcriptomic and proteomic datasets. However, this overlap was not preserved within statistically dysregulated molecules (p value < 0.05, unadjusted). Only five genes—Hspa5, S100a6, Plp1, Slc24a2, and Uggt1—were commonly dysregulated at both the mRNA and protein levels (Figure 4 A-B). In addition to the complexity of EVs, this limited concordance likely reflects the influence of posttranscriptional and posttranslational regulatory mechanisms, including mRNA stability, translational efficiency, and protein turnover, which are well documented contributors to the discordance between transcriptomic and proteomic data.

Among the enriched pathways identified independently from the transcriptomic and proteomic datasets, protein processing in the endoplasmic reticulum was the only pathway common to both analyses. Interestingly, within this pathway, Hspa5 is upregulated at both the mRNA and protein levels in response to morphine exposure in BDEVs, suggesting conserved stress–response activation [26,27]. In contrast, other transcripts contributing to this pathway were upregulated at the mRNA level, while their corresponding proteins were downregulated, further supporting the role of translational regulation or differential protein degradation in shaping the exosomal proteome under the influence of morphine (Figure 4 C-D) [28,29].

Morphine-BDEVs modulate neurodegenerative gene expression and activate opioid signaling in cross-species recipient neurons

To investigate the functional role of BDEVs and their potential to modulate neurodegenerative processes, we treated primary neurons with morphine-BDEVs and control-BDEVs, followed by a comprehensive multiplex gene expression analysis targeting 770 neuropathology-associated genes **(Fig. 5A)**. After controlling for multiple comparisons, we identified significant differential expression of 15 genes in primary neuronal cells following treatment with morphine-derived BDEVs (FDR q value < 0.1). Among these genes, *Mnat1*, a gene implicated in blood–brain barrier (BBB) damage in Alzheimer's disease (AD), was downregulated, whereas *PSEN1*, *NSF*, and *NRG1*, which are associated with neurodegenerative processes, particularly in AD, were upregulated **(Fig. 5B)**. This evidence supports previous findings suggesting that extracellular vesicles (EVs) may contribute to the neurodegeneration and dementia observed with long-term opioid use [30].

Pathway analysis revealed a selective enrichment of non-canonical WNT signaling components in neurons exposed to BDEVs derived from morphine-treated rats, despite the absence of direct morphine exposure. The top-ranked pathway was "Ca^{2+} pathway" (FDR = 2.75×10^{-6}; ratio = 0.005), followed by "Beta-catenin independent WNT signaling" (FDR = 5.71×10^{-5}; ratio = 0.01), and "Signaling by WNT" (FDR = 1.64×10^{-4}; ratio = 0.02). These non-canonical pathways are critical for cytoskeleton remodeling, intracellular calcium flux, and neuronal polarity. Remarkably, neurons also showed enrichment for "DARPP-32 events" and "Opioid signalling" (both FDR = 0.004), indicating activation of dopaminergic integration and GPCR-related neuromodulatory cascades. These results suggest that morphine-induced BDEVs can transfer biologically active signals capable of reprogramming recipient neurons toward a phenotype consistent with drug exposure, engaging both polarity-regulating pathways and classical neuroadaptive circuits **(Fig. 5C)**.

Discussion

This study identifies BDEVs as active participants in the cascade of neuroadaptations induced by chronic opioid exposure. Using an integrative omics approach, we show that morphine reprograms the transcriptomic and proteomic cargo of BDEVs in the rat PFC, enriching them with molecules linked to synaptic plasticity, endoplasmic reticulum (ER) stress, mitochondrial dysfunction, and neurodegenerative processes. Importantly, functional assays demonstrated that BDEVs derived from morphine-treated animals were sufficient to alter transcriptional programs in naïve cortical neurons, including genes involved in excitability and structural remodelling. These findings advance our understanding of OUD pathophysiology by implicating vesicle-mediated intercellular communication as a novel mechanism of drug-induced plasticity.

BDEVs as mediators of opioid-induced neuroadaptations

Addiction is widely recognized as a disorder of maladaptive plasticity, where repeated drug exposure induces long-lasting changes in brain circuits that regulate reward, cognition, and stress [31,32]. The PFC is a central hub for such adaptations, integrating glutamatergic and GABAergic inputs to modulate drug-seeking behaviour [33,34]. Our results demonstrate that chronic morphine alters the cargo of PFC-derived BDEVs, including transcripts and proteins central to synaptic remodelling (e.g., ARC, NCAM1), ER stress (Hspa5), and mitochondrial function (NDUF family) [35-37]. This suggests that opioids reshape not only intracellular

signalling cascades but also vesicle-mediated communication between neural cell types, adding a new layer to established models of opioid-induced neuroplasticity.

The identification of ARC gene as a consistently upregulated molecule in BDEVs of animals treated with morphine is particularly significant. ARC is an important regulator of synaptic plasticity and has been linked to drug-induced synaptic remodelling in several brain regions, including PFC [36,38]. ARC has also been implicated in the biogenesis and release of EVs. It can self-assemble into mRNA-containing, virus-like capsids that are packaged into EVs and released by neurons, where they can be endocytosed by recipient cells at postsynaptic sites [13,39,40]. Thus, the selective enrichment of ARC in BDEVs suggests a mechanism by which morphine-exposed neurons may broadcast plasticity-related signals to neighbouring cells, thereby coordinating circuit-wide adaptations [40]. Similarly, upregulation of Hspa5 in vesicles aligns with previous studies showing opioid-induced ER stress in mesocorticolimbic structures, which has been implicated in tolerance and dependence [41-44]. Together, these findings support the notion that vesicles carry molecular cargo that reflects and potentially amplifies core processes driving OUD.

Relationship to previous EV studies in opioid exposure

Previous research on EVs in the context of opioid exposure has primarily focused on peripheral vesicles, particularly blood-derived EVs enriched in microRNAs. For instance, opioid exposure has been associated with altered circulating miRNA profiles in both humans and animal models, while perinatal opioid exposure has been shown to modulate EV-associated small RNAs in the developing brain [45-47]. However, these studies were largely restricted to small RNA species, limiting insights into the broader transcript diversity of EVs, including messenger RNAs [48].

In contrast, our approach employed total RNA sequencing with ribosomal RNA removal, enabling the identification of mRNAs within BDEVs, consistent with recent evidence demonstrating the functional transfer of mRNAs via EVs [12], along with unbiased proteomic profiling. We further validated functional relevance by showing that morphine-altered BDEVs can reprogram transcriptional activity in recipient neurons. This extends beyond biomarker discovery, establishing BDEVs as active effectors of opioid-induced neuroadaptation.

Moreover, cross-referencing our RNA-seq data with a large-scale human GWAS meta-analysis for opioid use disorder revealed an overlap between morphine-altered vesicle cargo and genes associated with OUD, possibly underscoring the translational relevance of our

findings [15]. Transcripts such as Oprm1, Ncam1, and Kcnn1 not only play established roles in synaptic function and neuronal excitability but also appear within genetic risk loci for OUD, suggesting that BDEV cargo reflects both drug-induced molecular changes and intrinsic susceptibility pathways [15,49-51].

BDEV-mediated mechanisms of synaptic plasticity and circuit dysfunction in OUD

Our proteomic analyses further demonstrated significant alterations in the cargo of BDEVs following chronic morphine exposure, identifying dysregulated proteins implicated in neuroadaptations associated with opioid exposure. Specifically, we observed increased levels of PDIA3, STX1B, YWHAG, and HSPA5, molecules previously associated with synaptic dysfunction and pathways relevant to neurodegenerative diseases [52-55]. These findings align with previous evidence suggesting that prolonged opioid exposure may elevate the risk of neurodegeneration through mechanisms involving extracellular vesicles [56]. For instance, increased levels of neurodegeneration-related protein biomarkers have been detected in EVs isolated from the plasma of monkeys exposed to oxycodone [46]. Similarly, morphine-treated astrocytes have been shown to secrete EVs enriched with amyloid-related proteins, contributing to neurodegenerative processes in vitro [57].

Our pathway enrichment analyses across both proteomic and transcriptomic datasets revealed alterations in biological processes critical for synaptic remodelling, including axon guidance, lysosomal activity, and ER stress [58]. Alterations in axon guidance molecules have been reported in animal models of oxycodone self-administration, suggesting that vesicle-mediated signalling could contribute to aberrant synaptic connectivity and neuroplastic remodelling [59]. Likewise, the enrichment of ER stress pathways supports the hypothesis that opioid-induced plasticity involves maladaptive cellular stress responses [60].

Beyond ER stress, our analyses also revealed alterations in mitochondrial pathways, suggesting that morphine-evoked vesicle remodelling may broadly impact cellular energy metabolism. Notably, we observed enrichment of mitochondrial proteins such as COX1, COX7A2L, and NDUF subunits within BDEVs, suggesting that vesicle-mediated signalling may link opioid exposure to bioenergetic stress [61-63]. Mitochondrial dysfunction and oxidative damage are well-established consequences of chronic opioid use and have been implicated in both tolerance and neurotoxicity [22,64]. The selective export of mitochondrial proteins through BDEVs may reflect ongoing metabolic stress and could propagate vulnerability signals to neighbouring cells, thereby amplifying circuit dysfunction [65].

This interpretation is supported by our functional assays, which demonstrated that morphine-derived BDEVs were sufficient to induce transcriptional changes in naïve neurons consistent with neuroadaptive processes. A targeted gene expression panel revealed significant alterations in several neuropathology-associated genes, including upregulation of Psen1, Nsf, and Negr1, genes linked to neuronal connectivity, synaptic plasticity, and neurotransmitter signalling [66-68]. These findings indicate that morphine-BDEVs can trigger transcriptional programs aligned with neuroadaptive signatures. Pathway-level analysis further identified activation of opioid signalling and DARPP-32 cascades, as well as non-canonical WNT and calcium pathways associated with spine remodelling [69-71]. Collectively, these results suggest that BDEVs act as vehicles of synaptic reprogramming, transmitting drug-induced plasticity signals in the absence of direct receptor activation.

Translational implications: BDEVs as biomarkers and therapeutic targets

The ability of BDEVs to encapsulate and transmit opioid-induced molecular signatures has important translational implications. First BDEV cargo may serve as a biomarker for OUD. Because EVs can cross the blood–brain barrier and be isolated from peripheral fluids, profiling vesicle cargo could provide a minimally invasive means to monitor brain changes associated with opioid exposure [72]. Second, vesicle-mediated communication may represent a novel therapeutic target. Strategies aimed at modulating EV release, uptake, or cargo loading have shown promise in other disease contexts [73-75]. If BDEVs are found to amplify or sustain maladaptive signaling in vivo, interventions that alter vesicle biology could mitigate drug-induced neuroadaptations [72]. For example, targeting ER stress pathways (e.g., Hspa5) or synaptic regulators (e.g., ARC) within vesicles may reduce the persistence of opioid-induced plasticity

In conclusion, our findings identify BDEVs as active mediators of opioid-induced neuroplasticity. Chronic morphine exposure reprograms vesicle cargo at both transcriptomic and proteomic levels, enriching molecules involved in synaptic plasticity, stress responses, and mitochondrial function. These vesicles are not passive byproducts, but are capable of reprogramming recipient neurons, thereby contributing to the persistence of drug-induced adaptations. By linking BDEVs biology with addiction neuroscience, this work advances mechanistic understanding of OUD and highlights possible new opportunities for biomarker discovery and therapeutic intervention.

Authors Contribution

PHG and RGO designed the study. PHG, SB, RR, FC, and NRS performed experiments and data acquisition. MRL and VCC conducted proteomic analyses. YY and TWV contributed to RNA sequencing and data processing. TB performed TB performed transmission electron microscopy. CBV, HKM, SJ, RGO provided supervision, resources, and critical input on experimental design and interpretation. RGO conceived the project, secured funding. PHG and RGO wrote the manuscript with input from all authors. All authors reviewed and approved the final version

Funding

This work was supported by the Independent Research Fund Denmark (DFF, grant no. 3166-00139B) and by the Brazilian National Council for Scientific and Technological Development (CNPq, grant nos. 444358/2024-2, 401678/2022-9, and 306580/2022-5), all awarded to Dr. Rodrigo Grassi-Oliveira (RGO).

Competing Interests

All authors report no biomedical financial interests or potential conflicts of interest.

References

1 Fairley M, Humphreys K, Joyce VR, Bounthavong M, Trafton J, Combs A, et al. Cost-effectiveness of Treatments for Opioid Use Disorder. JAMA Psychiatry. 2021;78(7):767–77.
2 Kreek MJ, Levran O, Reed B, Schlussman SD, Zhou Y, Butelman ER. Opiate addiction and cocaine addiction: underlying molecular neurobiology and genetics. J Clin Invest. 2012;122(10):3387–93.
3 Gold MS, Baron D, Bowirrat A, Blum K. Neurological correlates of brain reward circuitry linked to opioid use disorder (OUD): Do homo sapiens acquire or have a reward deficiency syndrome? J Neurol Sci. 2020;418:117137.
4 Manglik A. Molecular Basis of Opioid Action: From Structures to New Leads. Biol Psychiatry. 2020;87(1):6–14.
5 Gruner HN, McManus MT. Examining the evidence for extracellular RNA function in mammals. Nat Rev Genet. 2021;22(7):448–58.
6 Antonucci F, Turola E, Riganti L, Caleo M, Gabrielli M, Perrotta C, et al. Microvesicles released from microglia stimulate synaptic activity via enhanced sphingolipid metabolism. EMBO J. 2012;31(5):1231–40.
7 Li K, Wang K, Xu SX, Xie XH, Tang Y, Zhang L, et al. Investigating Neuroplasticity Changes Reflected by BDNF Levels in Astrocyte-Derived Extracellular Vesicles in Patients with Depression. Int J Nanomedicine. 2024;19:8971–85.

8 Filannino FM, Panaro MA, Benameur T, Pizzolorusso I, Porro C. Extracellular Vesicles in the Central Nervous System: A Novel Mechanism of Neuronal Cell Communication. Int J Mol Sci. 2024;25(3).
9 Chivero ET, Dagur RS, Peeples ES, Sil S, Liao K, Ma R, et al. Biogenesis, physiological functions and potential applications of extracellular vesicles in substance use disorders. Cell Mol Life Sci. 2021;78(11):4849–65.
10 O'Brien K, Breyne K, Ughetto S, Laurent LC, Breakefield XO. RNA delivery by extracellular vesicles in mammalian cells and its applications. Nat Rev Mol Cell Biol. 2020;21(10):585–606.
11 Dellar ER, Hill C, Melling GE, Carter DRF, Baena-Lopez LA. Unpacking extracellular vesicles: RNA cargo loading and function. J Extracell Biol. 2022;1(5):e40.
12 Ransom LS, Liu CS, Dunsmore E, Palmer CR, Nicodemus J, Ziomek D, et al. Human brain small extracellular vesicles contain selectively packaged, full-length mRNA. Cell Rep. 2024;43(4):114061.
13 Pastuzyn ED, Day CE, Kearns RB, Kyrke-Smith M, Taibi AV, McCormick J, et al. The Neuronal Gene Arc Encodes a Repurposed Retrotransposon Gag Protein that Mediates Intercellular RNA Transfer. Cell. 2018;172(1-2):275–88 e18.
14 D'Acunzo P, Kim Y, Ungania JM, Perez-Gonzalez R, Goulbourne CN, Levy E. Isolation of mitochondria-derived mitovesicles and subpopulations of microvesicles and exosomes from brain tissues. Nat Protoc. 2022;17(11):2517–49.
15 Kember RL, Vickers-Smith R, Xu H, Toikumo S, Niarchou M, Zhou H, et al. Cross-ancestry meta-analysis of opioid use disorder uncovers novel loci with predominant effects in brain regions associated with addiction. Nat Neurosci. 2022;25(10):1279–87.
16 Zhang B, Wang J, Wang X, Zhu J, Liu Q, Shi Z, et al. Proteogenomic characterization of human colon and rectal cancer. Nature. 2014;513(7518):382–7.
17 Cox J, Mann M. MaxQuant enables high peptide identification rates, individualized p.p.b.-range mass accuracies and proteome-wide protein quantification. Nat Biotechnol. 2008;26(12):1367–72.
18 Thery C, Witwer KW, Aikawa E, Alcaraz MJ, Anderson JD, Andriantsitohaina R, et al. Minimal information for studies of extracellular vesicles 2018 (MISEV2018): a position statement of the International Society for Extracellular Vesicles and update of the MISEV2014 guidelines. J Extracell Vesicles. 2018;7(1):1535750.
19 Li M, Zeringer E, Barta T, Schageman J, Cheng A, Vlassov AV. Analysis of the RNA content of the exosomes derived from blood serum and urine and its potential as biomarkers. Philos Trans R Soc Lond B Biol Sci. 2014;369(1652).
20 Kanehisa M, Sato Y, Furumichi M, Morishima K, Tanabe M. New approach for understanding genome variations in KEGG. Nucleic Acids Res. 2019;47(D1):D590–D95.
21 Lin MT, Beal MF. Mitochondrial dysfunction and oxidative stress in neurodegenerative diseases. Nature. 2006;443(7113):787–95.
22 Federico A, Cardaioli E, Da Pozzo P, Formichi P, Gallus GN, Radi E. Mitochondria, oxidative stress and neurodegeneration. J Neurol Sci. 2012;322(1-2):254–62.
23 Wallace DC. Mitochondrial genetic medicine. Nat Genet. 2018;50(12):1642–49.
24 Niswender CM, Conn PJ. Metabotropic glutamate receptors: physiology, pharmacology, and disease. Annu Rev Pharmacol Toxicol. 2010;50:295–322.
25 Trantham-Davidson H, Chandler LJ. Alcohol-induced alterations in dopamine modulation of prefrontal activity. Alcohol. 2015;49(8):773–9.

26 Lee AS. The glucose-regulated proteins: stress induction and clinical applications. Trends Biochem Sci. 2001;26(8):504–10.
27 Chen X, Shi C, He M, Xiong S, Xia X. Endoplasmic reticulum stress: molecular mechanism and therapeutic targets. Signal Transduct Target Ther. 2023;8(1):352.
28 Tyanova S, Temu T, Cox J. The MaxQuant computational platform for mass spectrometry-based shotgun proteomics. Nat Protoc. 2016;11(12):2301–19.
29 Jung M, Lee EK. RNA-Binding Protein HuD as a Versatile Factor in Neuronal and Non-Neuronal Systems. Biology (Basel). 2021;10(5).
30 Morris DC, Zacharek A, Zhang ZG, Chopp M. Extracellular vesicles-Mediators of opioid use disorder? Addict Biol. 2023;28(12):e13353.
31 Kourrich S, Calu DJ, Bonci A. Intrinsic plasticity: an emerging player in addiction. Nat Rev Neurosci. 2015;16(3):173–84.
32 Kalivas PW, O'Brien C. Drug addiction as a pathology of staged neuroplasticity. Neuropsychopharmacology. 2008;33(1):166–80.
33 Koob GF, Volkow ND. Neurocircuitry of addiction. Neuropsychopharmacology. 2010;35(1):217–38.
34 Cole RH, Moussawi K, Joffe ME. Opioid modulation of prefrontal cortex cells and circuits. Neuropharmacology. 2024;248:109891.
35 Sytnyk V, Leshchyns'ka I, Nikonenko AG, Schachner M. NCAM promotes assembly and activity-dependent remodeling of the postsynaptic signaling complex. J Cell Biol. 2006;174(7):1071–85.
36 Korb E, Finkbeiner S. Arc in synaptic plasticity: from gene to behavior. Trends Neurosci. 2011;34(11):591–8.
37 Ajoolabady A, Lindholm D, Ren J, Pratico D. ER stress and UPR in Alzheimer's disease: mechanisms, pathogenesis, treatments. Cell Death Dis. 2022;13(8):706.
38 McReynolds JR, Holloway-Erickson CM, Parmar TU, McIntyre CK. Corticosterone-induced enhancement of memory and synaptic Arc protein in the medial prefrontal cortex. Neurobiol Learn Mem. 2014;112:148–57.
39 Ashley J, Cordy B, Lucia D, Fradkin LG, Budnik V, Thomson T. Retrovirus-like Gag Protein Arc1 Binds RNA and Traffics across Synaptic Boutons. Cell. 2018;172(1-2):262–74 e11.
40 Hantak MP, Einstein J, Kearns RB, Shepherd JD. Intercellular Communication in the Nervous System Goes Viral. Trends Neurosci. 2021;44(4):248–59.
41 Looschen K, Jeffers A, Chakraborty S, Salisbury C, Dodge A, Hochstetler M, et al. Adolescent stress avoidance influences cue-induced heroin seeking and chaperonin gene expression in the dorsal striatum of adult female rats. Am J Drug Alcohol Abuse. 2025:1–9.
42 Lefevre EM, Pisansky MT, Toddes C, Baruffaldi F, Pravetoni M, Tian L, et al. Interruption of continuous opioid exposure exacerbates drug-evoked adaptations in the mesolimbic dopamine system. Neuropsychopharmacology. 2020;45(11):1781–92.
43 Ammon S, Mayer P, Riechert U, Tischmeyer H, Hollt V. Microarray analysis of genes expressed in the frontal cortex of rats chronically treated with morphine and after naloxone precipitated withdrawal. Brain Res Mol Brain Res. 2003;112(1-2):113–25.
44 Liu D, Zhou Y, Peng Y, Su P, Li Z, Xu Q, et al. Endoplasmic Reticulum Stress in Spinal Cord Contributes to the Development of Morphine Tolerance. Front Mol Neurosci. 2018;11:72.
45 Chen F, Zou L, Dai Y, Sun J, Chen C, Zhang Y, et al. Prognostic plasma exosomal microRNA biomarkers in patients with substance use disorders presenting comorbid with anxiety and depression. Sci Rep. 2021;11(1):6271.

46 Kumar A, Kim S, Su Y, Sharma M, Kumar P, Singh S, et al. Brain cell-derived exosomes in plasma serve as neurodegeneration biomarkers in male cynomolgus monkeys self-administrating oxycodone. EBioMedicine. 2021;63:103192.
47 Shahjin F, Guda RS, Schaal VL, Odegaard K, Clark A, Gowen A, et al. Brain-Derived Extracellular Vesicle microRNA Signatures Associated with In Utero and Postnatal Oxycodone Exposure. Cells. 2019;9(1).
48 Miceli RT, Chen TY, Nose Y, Tichkule S, Brown B, Fullard JF, et al. Extracellular vesicles, RNA sequencing, and bioinformatic analyses: Challenges, solutions, and recommendations. J Extracell Vesicles. 2024;13(12):e70005.
49 Johnson ECB, Bian S, Haque RU, Carter EK, Watson CM, Gordon BA, et al. Cerebrospinal fluid proteomics define the natural history of autosomal dominant Alzheimer's disease. Nat Med. 2023;29(8):1979–88.
50 Li L, Cao J, Zhang S, Wang C, Wang J, Song G, et al. NCAM signaling mediates the effects of GDNF on chronic morphine-induced neuroadaptations. J Mol Neurosci. 2014;53(4):580–9.
51 Kshatri AS, Gonzalez-Hernandez A, Giraldez T. Physiological Roles and Therapeutic Potential of Ca(2+) Activated Potassium Channels in the Nervous System. Front Mol Neurosci. 2018;11:258.
52 Cassano T, Giamogante F, Calcagnini S, Romano A, Lavecchia AM, Inglese F, et al. PDIA3 Expression Is Altered in the Limbic Brain Regions of Triple-Transgenic Mouse Model of Alzheimer's Disease. Int J Mol Sci. 2023;24(3).
53 Mishima T, Fujiwara T, Kofuji T, Saito A, Terao Y, Akagawa K. Syntaxin 1B regulates synaptic GABA release and extracellular GABA concentration, and is associated with temperature-dependent seizures. J Neurochem. 2021;156(5):604–13.
54 Enogieru AB, Omoruyi SI, Hiss DC, Ekpo OE. GRP78/BIP/HSPA5 as a Therapeutic Target in Models of Parkinson's Disease: A Mini Review. Adv Pharmacol Sci. 2019;2019:2706783.
55 Oh HS, Urey DY, Karlsson L, Zhu Z, Shen Y, Farinas A, et al. A cerebrospinal fluid synaptic protein biomarker for prediction of cognitive resilience versus decline in Alzheimer's disease. Nat Med. 2025;31(5):1592–603.
56 Venkatesan S, Binko MA, Mielnik CA, Ramsey AJ, Lambe EK. Deficits in integrative NMDA receptors caused by Grin1 disruption can be rescued in adulthood. Neuropsychopharmacology. 2023;48(12):1742–51.
57 Sil S, Singh S, Chemparathy DT, Chivero ET, Gordon L, Buch S. Astrocytes & Astrocyte derived Extracellular Vesicles in Morphine Induced Amyloidopathy: Implications for Cognitive Deficits in Opiate Abusers. Aging Dis. 2021;12(6):1389–408.
58 Dacher M, Nugent FS. Opiates and plasticity. Neuropharmacology. 2011;61(7):1088–96.
59 Yuferov V, Zhang Y, Liang Y, Zhao C, Randesi M, Kreek MJ. Oxycodone Self-Administration Induces Alterations in Expression of Integrin, Semaphorin and Ephrin Genes in the Mouse Striatum. Front Psychiatry. 2018;9:257.
60 Cai Y, Yang L, Hu G, Chen X, Niu F, Yuan L, et al. Regulation of morphine-induced synaptic alterations: Role of oxidative stress, ER stress, and autophagy. J Cell Biol. 2016;215(2):245–58.
61 Mimaki M, Wang X, McKenzie M, Thorburn DR, Ryan MT. Understanding mitochondrial complex I assembly in health and disease. Biochim Biophys Acta. 2012;1817(6):851–62.
62 Mick DU, Fox TD, Rehling P. Inventory control: cytochrome c oxidase assembly regulates mitochondrial translation. Nat Rev Mol Cell Biol. 2011;12(1):14–20.

63 Perez-Perez R, Lobo-Jarne T, Milenkovic D, Mourier A, Bratic A, Garcia-Bartolome A, et al. COX7A2L Is a Mitochondrial Complex III Binding Protein that Stabilizes the III2+IV Supercomplex without Affecting Respirasome Formation. Cell Rep. 2016;16(9):2387–98.
64 Sun E, Torices S, Osborne OM, Toborek M. Microvascular Dysfunction, Mitochondrial Reprogramming, and Inflammasome Activation as Critical Regulators of Ischemic Stroke Severity Induced by Chronic Exposure to Prescription Opioids. J Neurosci. 2025;45(8).
65 Di Mambro T, Pellielo G, Agyapong ED, Carinci M, Chianese D, Giorgi C, et al. The Tricky Connection between Extracellular Vesicles and Mitochondria in Inflammatory-Related Diseases. Int J Mol Sci. 2023;24(9).
66 Maksour S, Finol-Urdaneta RK, Hulme AJ, Cabral-da-Silva MEC, Targa Dias Anastacio H, Balez R, et al. Alzheimer's disease induced neurons bearing PSEN1 mutations exhibit reduced excitability. Front Cell Neurosci. 2024;18:1406970.
67 Su F, Pfundstein G, Sah S, Zhang S, Keable R, Hagan DW, et al. Neuronal growth regulator 1 (NEGR1) promotes the synaptic targeting of glutamic acid decarboxylase 65 (GAD65). J Neurochem. 2025;169(1):e16279.
68 Zhao C, Slevin JT, Whiteheart SW. Cellular functions of NSF: not just SNAPs and SNAREs. FEBS Lett. 2007;581(11):2140–9.
69 Greener MR, Storr SJ. Exploring the Role of DARPP-32 in Addiction: A Review of the Current Limitations of Addiction Treatment Pathways and the Role of DARPP-32 to Improve Them. NeuroSci. 2022;3(3):494–509.
70 Wu M, Li Z, Liang L, Ma P, Cui D, Chen P, et al. Wnt signaling contributes to withdrawal symptoms from opioid receptor activation induced by morphine exposure or chronic inflammation. Pain. 2020;161(3):532–44.
71 Reeves KC, Shah N, Munoz B, Atwood BK. Opioid Receptor-Mediated Regulation of Neurotransmission in the Brain. Front Mol Neurosci. 2022;15:919773.
72 Kumar S, El-Hage N, Batrakova E. Extracellular Vesicles in HIV, Drug Abuse, and Drug Delivery. J Neuroimmune Pharmacol. 2020;15(3):387–89.
73 Peruzzi JA, Gunnels TF, Edelstein HI, Lu P, Baker D, Leonard JN, et al. Enhancing extracellular vesicle cargo loading and functional delivery by engineering protein-lipid interactions. Nat Commun. 2024;15(1):5618.
74 Joshi BS, de Beer MA, Giepmans BNG, Zuhorn IS. Endocytosis of Extracellular Vesicles and Release of Their Cargo from Endosomes. ACS Nano. 2020;14(4):4444–55.
75 Li J, Wang J, Chen Z. Emerging role of exosomes in cancer therapy: progress and challenges. Mol Cancer. 2025;24(1):13.

Figure Legends

Figure 1. Characterization of BDEVs from rat prefrontal cortex.

(A) Experimental design. (B) Nanoparticle tracking analysis (NTA) showing no significant changes in concentration or size distribution of isolated BDEVs between groups.(C) Representative electron micrographs of EVs. (D) Western blot analysis confirming the presence

of EV markers Flotillin and HSP70, and absence of the exclusion marker GM130 in the EV samples.

Figure 2. Effect of morphine treatment on the RNA profile of BDEVs

(A) Volcano plot of differentially expressed mRNAs in BDEVs from morphine-treated versus control animals. (B) KEGG pathway enrichment analysis of morphine-induced RNA alterations. (C) Dot plot showing upregulated and downregulated transcripts within enriched pathways. (D) Heatmap of significantly dysregulated mRNAs across enriched pathways ($\log_2$ fold-change). (E) Network visualization of enriched pathways and associated transcripts. (F) Integration with a human GWAS for opioid use disorder highlights risk-associated genes differentially expressed in BDEVs. (G) RNA deconvolution estimates brain cell-type composition, with nearly 40% of transcripts inferred from GABAergic interneuron-derived BDEVs.

Figure 3. Effect of morphine treatment on the protein profile of BDEVs

(A) Volcano plot showing differentially expressed proteins in BDEVs from morphine-treated versus control animals. (B) Dynamic range of protein abundance (left) and MA plot (right), highlighting significantly dysregulated proteins. (C) KEGG pathway enrichment analysis identifying pathways associated with morphine-induced protein alterations. (D) Network visualization of enriched pathways and associated proteins. Gray nodes represent KEGG pathways; colored nodes represent proteins, with node color indicating $\log_2$ fold-change (red = upregulated, blue = downregulated). (E) Heatmap of $\log_2$ fold-change values for dysregulated proteins across enriched KEGG pathways.

Figure 4. Integrated transcriptomic and proteomic analysis of BDEVs from morphine-treated rats.

(A) Circos plot linking significantly dysregulated mRNAs (left) and proteins (right). Node colors represent $\log_2$ fold-change (red/orange = upregulated, blue = downregulated). (B) UpSet plot showing the overlap between significantly altered RNAs and proteins; bar height represents the number of molecules in each set. (C) Comparative KEGG pathway enrichment analysis of dysregulated mRNAs and proteins. Bubble size reflects the number of molecules per pathway, and color indicates $-\log_{10}(p)$. (D) Chord diagram of the protein processing in

endoplasmic reticulum pathway, depicting concordance and divergence between RNA and protein levels. Ribbons connect matched RNA–protein pairs, with ribbon color indicating $\log_2$ fold-change.

Figure 5. Effect of morphine-derived BDEVs on primary neuronal cultures. (A) Experimental design: BDEVs from morphine- and vehicle-treated rats were applied for 24 h to primary cortical neurons, followed by NanoString analysis. (B) Volcano plot showing differentially expressed transcripts in neurons exposed to morphine-derived BDEVs; selected significant genes are labeled. (C) Reactome pathway enrichment of dysregulated genes, highlighting Ca^{2+}, WNT, opioid, and DARP 32-related signaling pathways.

A

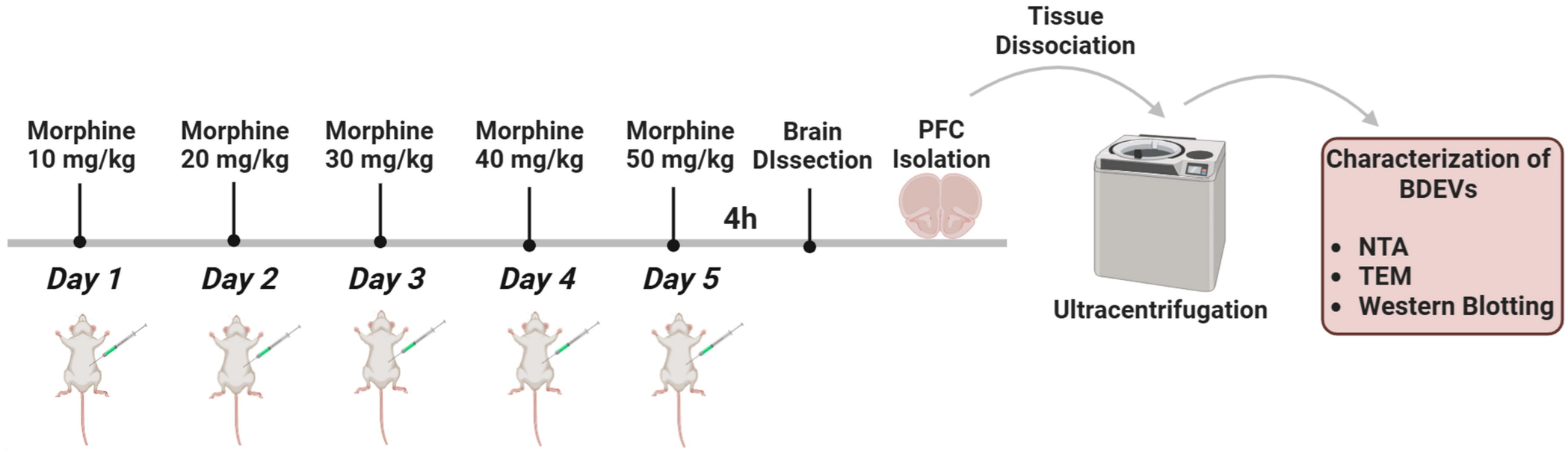
Morphine 10 mg/kg
Morphine 20 mg/kg
Morphine 30 mg/kg
Morphine 40 mg/kg
Morphine 50 mg/kg
Brain DIssection
PFC Isolation
4h
Day 1
Day 2
Day 3
Day 4
Day 5
Tissue Dissociation
Ultracentrifugation
Characterization of BDEVs
NTA
TEM
Western Blotting

B

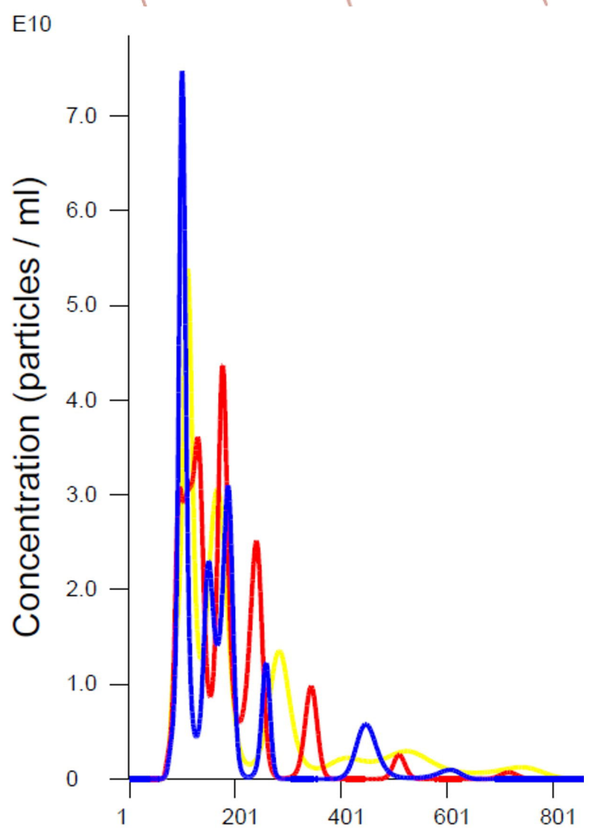
E10
Concentration (particles / ml)
7.0
6.0
5.0
4.0
3.0
2.0
1.0
0
1
201
401
601
801

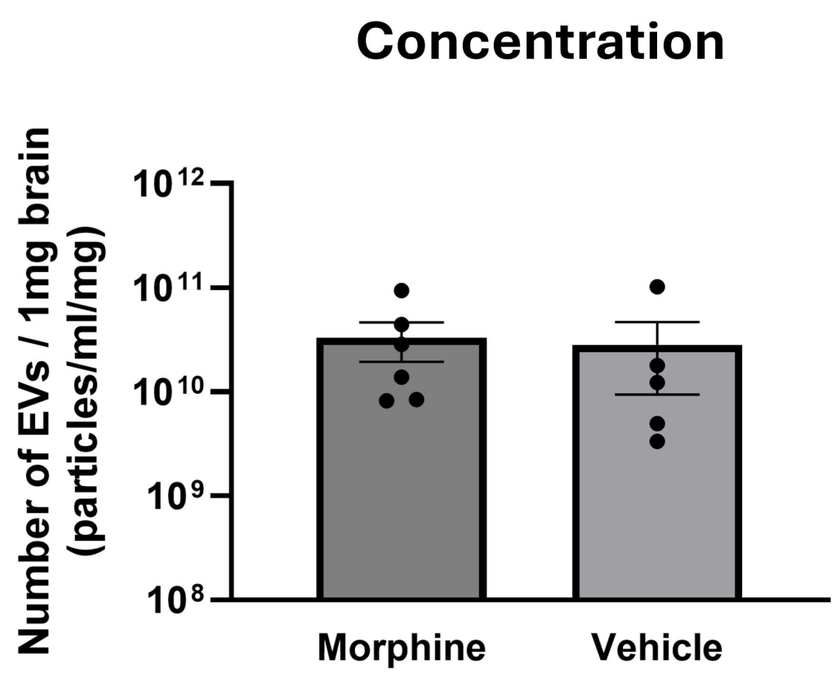
Concentration
Number of EVs / 1mg brain (particles/ml/mg)
10^{12}
10^{11}
10^{10}
10^{9}
10^{8}
Morphine
Vehicle

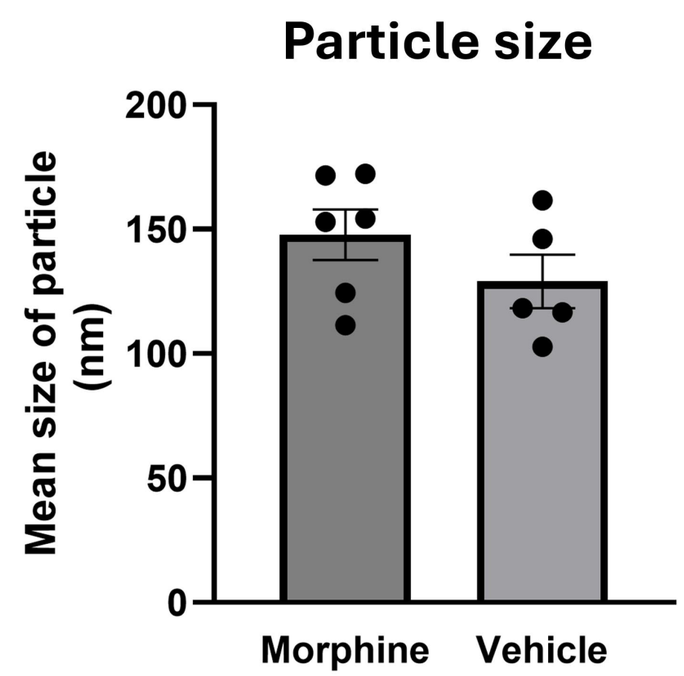
Particle size
Mean size of particle (nm)
200
150
100
50
0
Morphine
Vehicle

C

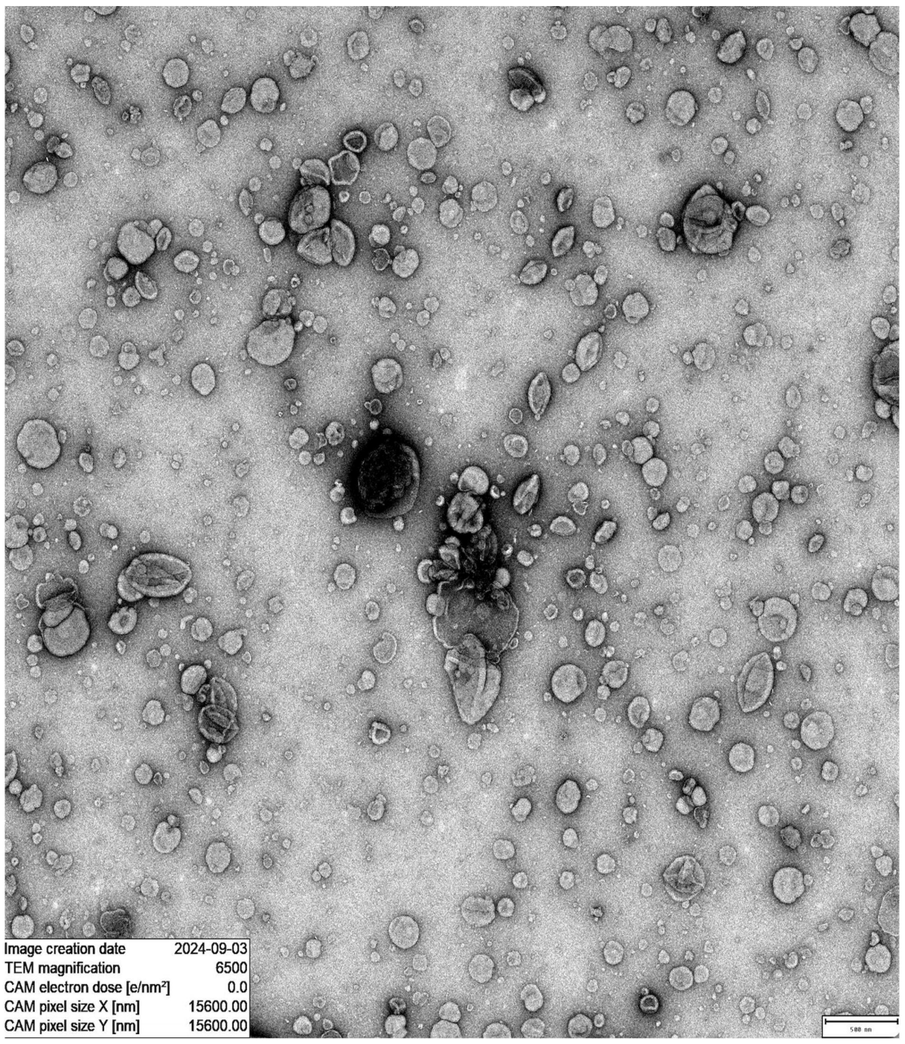
Image creation date 2024-09-03
TEM magnification 6500
CAM electron dose [e/nm²] 0.0
CAM pixel size X [nm] 15600.00
CAM pixel size Y [nm] 15600.00

D

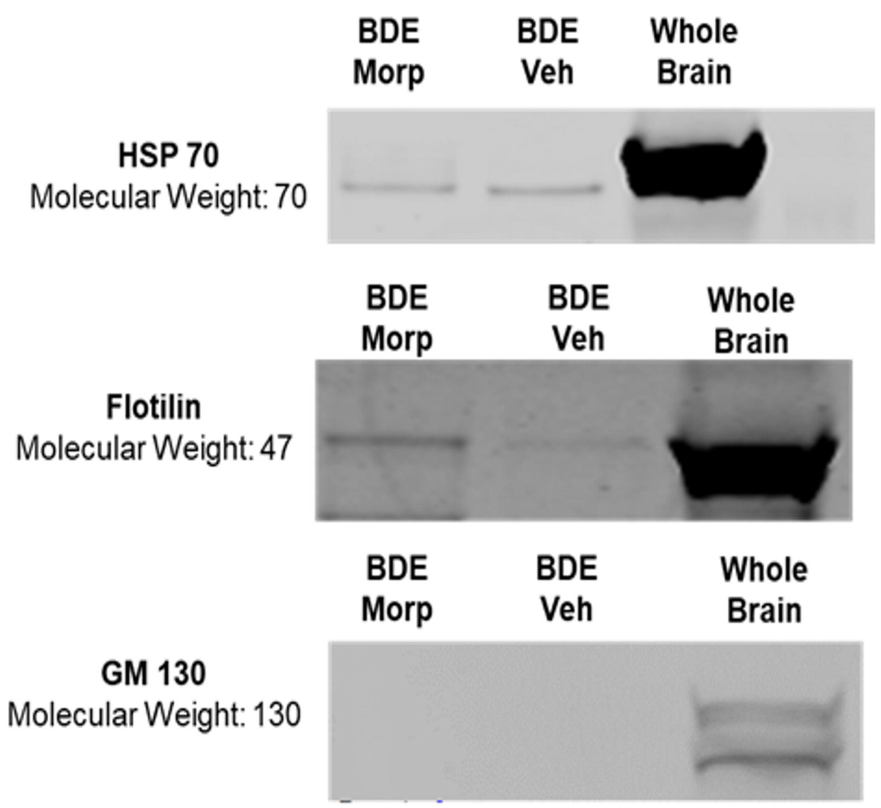
BDE Morp
BDE Veh
Whole Brain
HSP 70
Molecular Weight: 70
BDE Morp
BDE Veh
Whole Brain
Flotilin
Molecular Weight: 47
BDE Morp
BDE Veh
Whole Brain
GM 130
Molecular Weight: 130

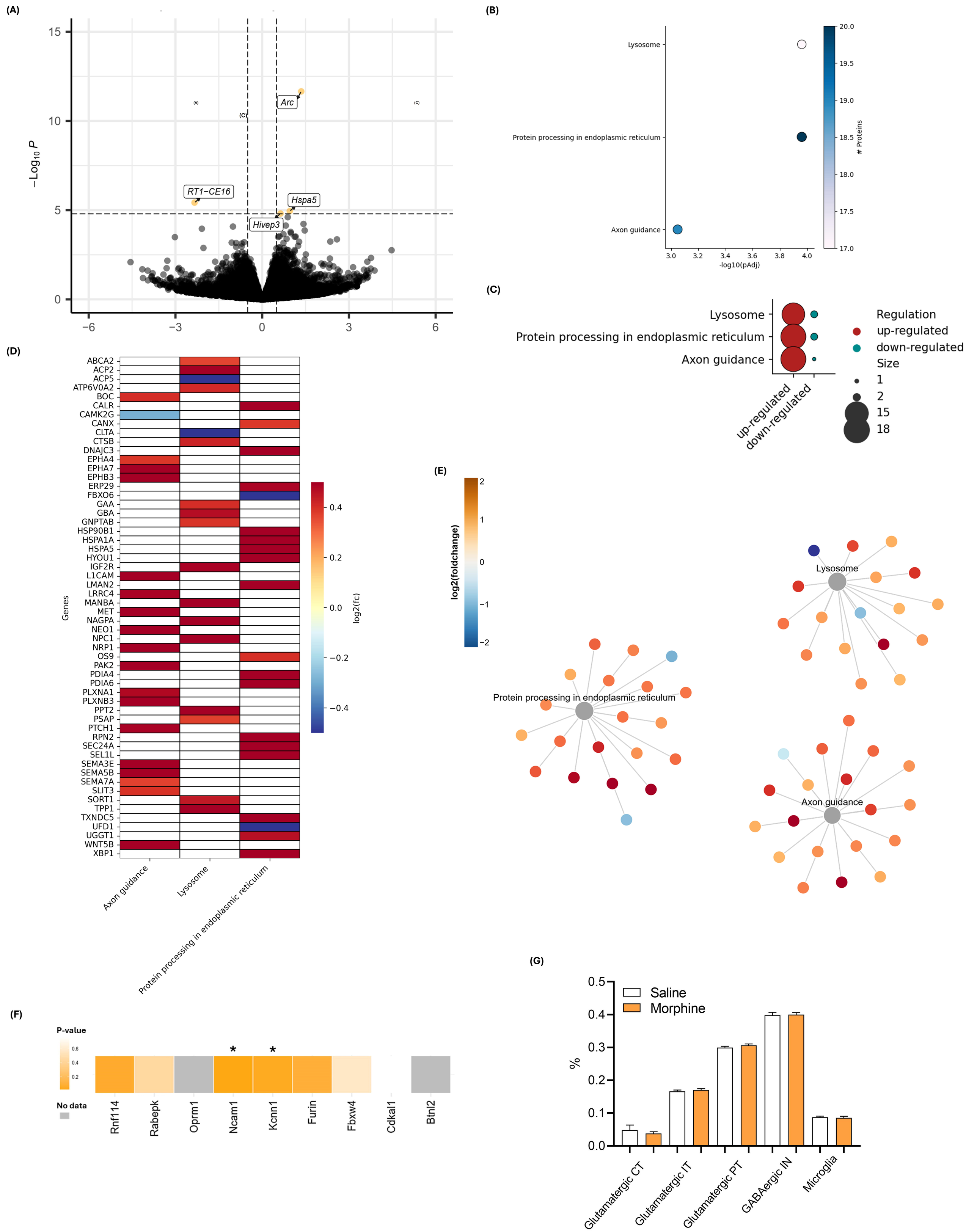
(A)
−Log10 P
Arc
RT1−CE16
Hspa5
Hivep3
(B)
Lysosome
Protein processing in endoplasmic reticulum
Axon guidance
-log10(pAdj)
Proteins
(C)
Lysosome
Protein processing in endoplasmic reticulum
Axon guidance
up-regulated
down-regulated
Regulation
up-regulated
down-regulated
Size
(D)
Genes
log2(fc)
Axon guidance
Lysosome
Protein processing in endoplasmic reticulum
(E)
log2(foldchange)
Lysosome
Protein processing in endoplasmic reticulum
Axon guidance
(F)
P-value
No data
Rnf114
Rabepk
Oprm1
Ncam1
Kcnn1
Furin
Fbxw4
Cdkal1
Btnl2
(G)
Saline
Morphine
%
Glutamatergic CT
Glutamatergic IT
Glutamatergic PT
GABAergic IN
Microglia

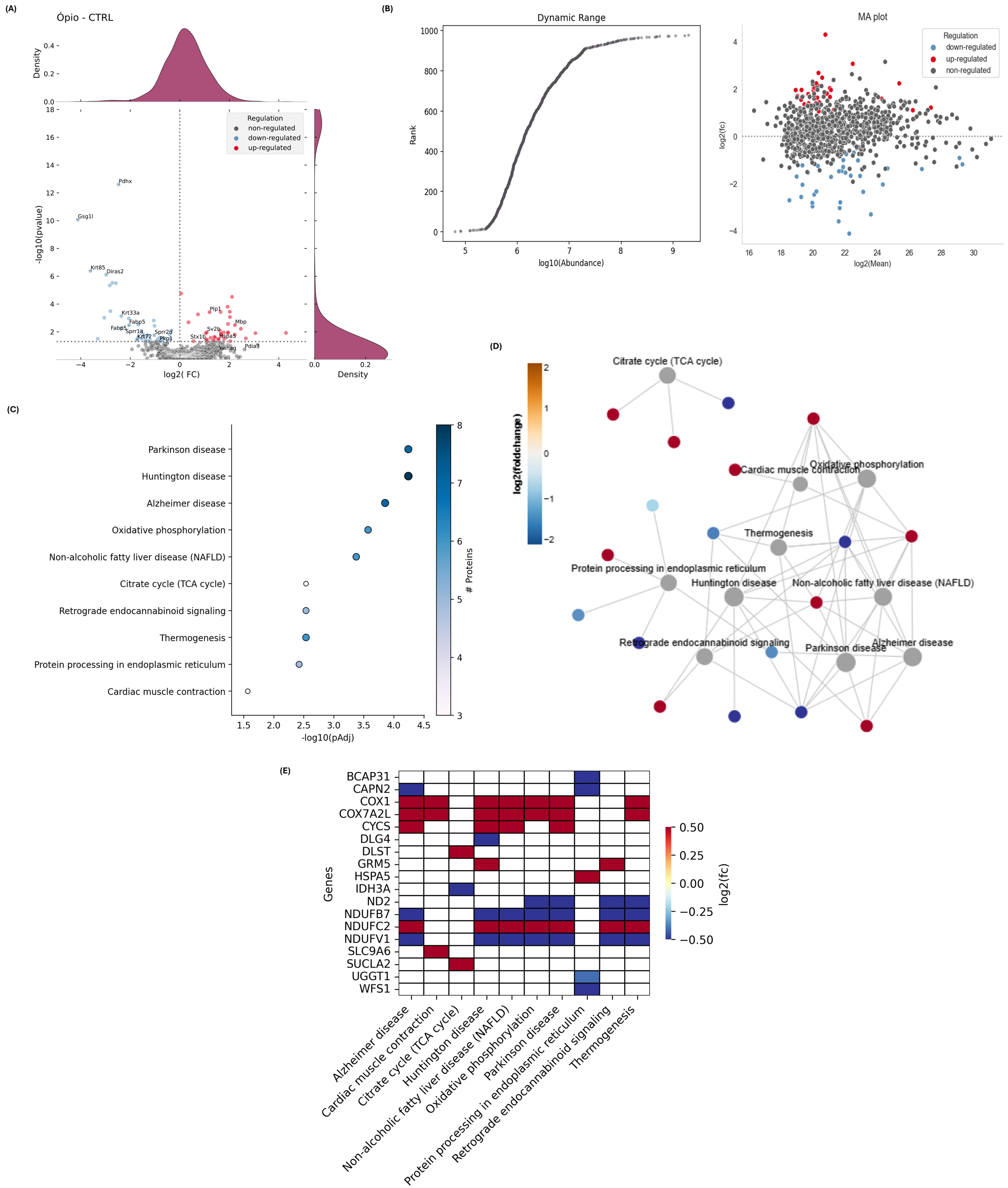
(A)
Ópio - CTRL
Density
Regulation
non-regulated
down-regulated
up-regulated
Pdhx
Gsg1l
Krt85
Diras2
Krt33a
Fabp5
Sprr1a
Sprr2d
Krt72
Pkp1
Plp1
Mbp
Sv2b
Stx1b
Hspa5
Ywhag
Pdia3
-log10(pvalue)
log2(FC)
(B)
Dynamic Range
Rank
log10(Abundance)
MA plot
Regulation
down-regulated
up-regulated
non-regulated
log2(fc)
log2(Mean)
(C)
Parkinson disease
Huntington disease
Alzheimer disease
Oxidative phosphorylation
Non-alcoholic fatty liver disease (NAFLD)
Citrate cycle (TCA cycle)
Retrograde endocannabinoid signaling
Thermogenesis
Protein processing in endoplasmic reticulum
Cardiac muscle contraction
-log10(pAdj)
Proteins
(D)
Citrate cycle (TCA cycle)
log2(foldchange)
Cardiac muscle contraction
Oxidative phosphorylation
Thermogenesis
Protein processing in endoplasmic reticulum
Huntington disease
Non-alcoholic fatty liver disease (NAFLD)
Retrograde endocannabinoid signaling
Parkinson disease
Alzheimer disease
(E)
Genes
BCAP31
CAPN2
COX1
COX7A2L
CYCS
DLG4
DLST
GRM5
HSPA5
IDH3A
ND2
NDUFB7
NDUFC2
NDUFV1
SLC9A6
SUCLA2
UGGT1
WFS1
Alzheimer disease
Cardiac muscle contraction
Citrate cycle (TCA cycle)
Huntington disease
Non-alcoholic fatty liver disease (NAFLD)
Oxidative phosphorylation
Parkinson disease
Protein processing in endoplasmic reticulum
Retrograde endocannabinoid signaling
Thermogenesis
log2(fc)

(A)

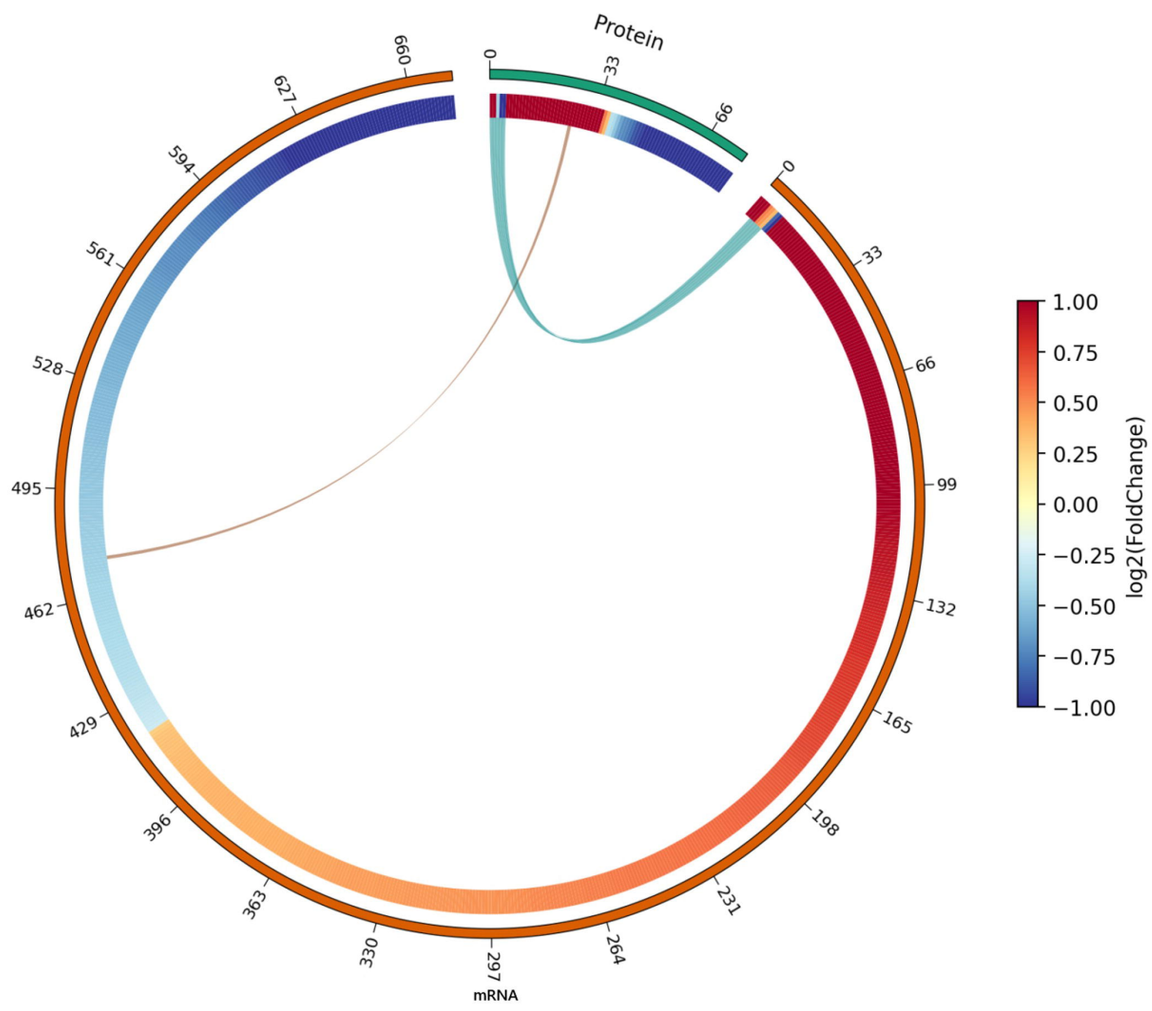
Protein
mRNA
660
627
594
561
528
495
462
429
396
363
330
297
264
231
198
165
132
99
66
33
0
1.00
0.75
0.50
0.25
0.00
−0.25
−0.50
−0.75
−1.00
log2(FoldChange)

(B)

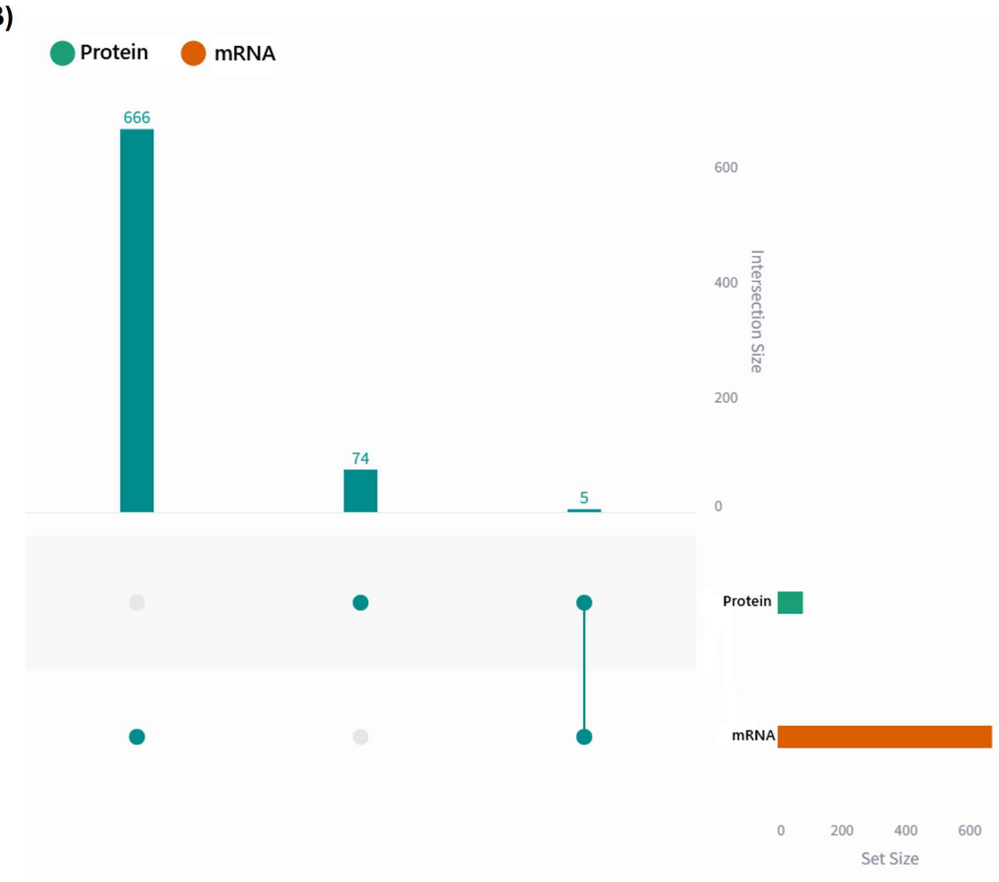
Protein
mRNA
666
74
5
Intersection Size
600
400
200
0
Protein
mRNA
0
200
400
600
Set Size

(C)

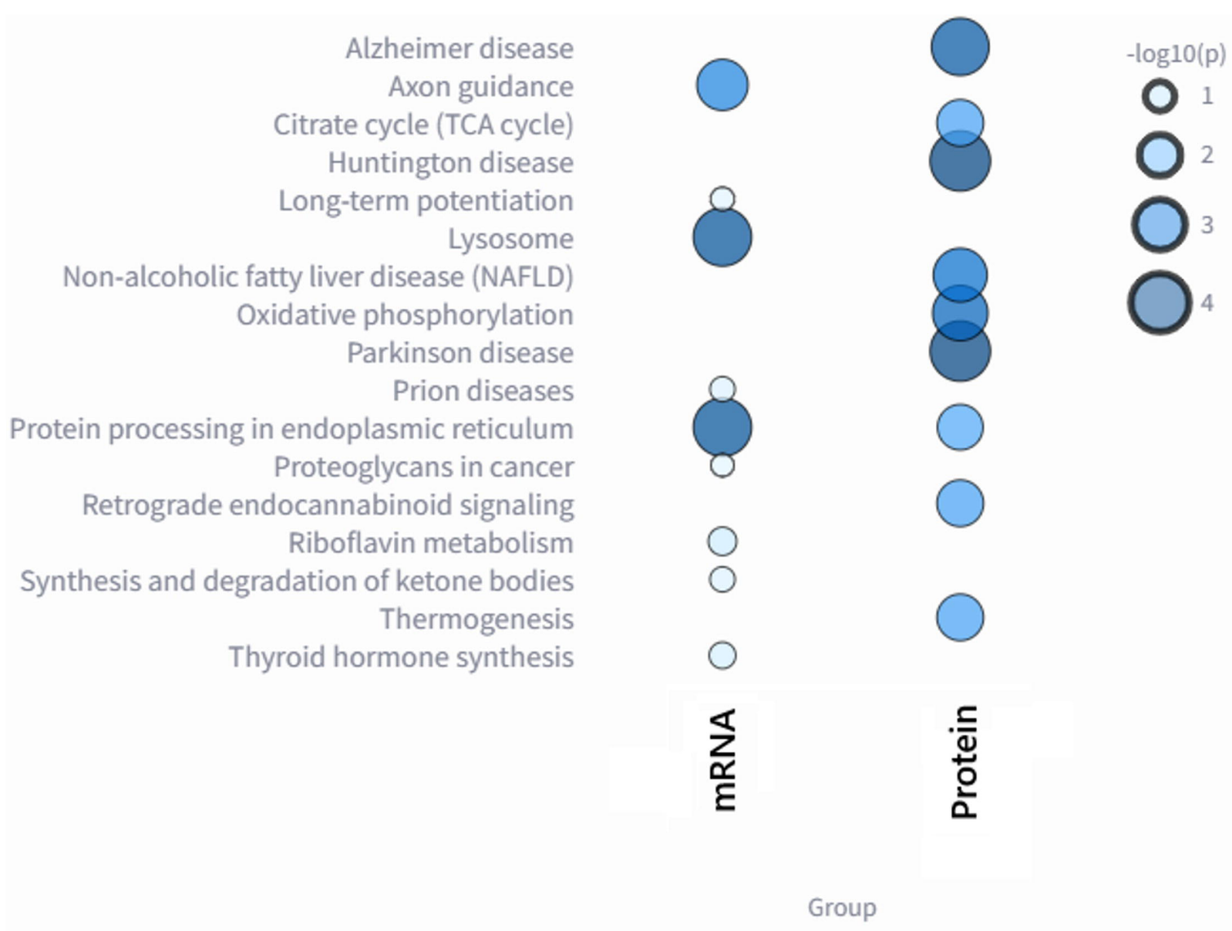
Alzheimer disease
Axon guidance
Citrate cycle (TCA cycle)
Huntington disease
Long-term potentiation
Lysosome
Non-alcoholic fatty liver disease (NAFLD)
Oxidative phosphorylation
Parkinson disease
Prion diseases
Protein processing in endoplasmic reticulum
Proteoglycans in cancer
Retrograde endocannabinoid signaling
Riboflavin metabolism
Synthesis and degradation of ketone bodies
Thermogenesis
Thyroid hormone synthesis
mRNA
Protein
Group
-log10(p)
1
2
3
4

(D)

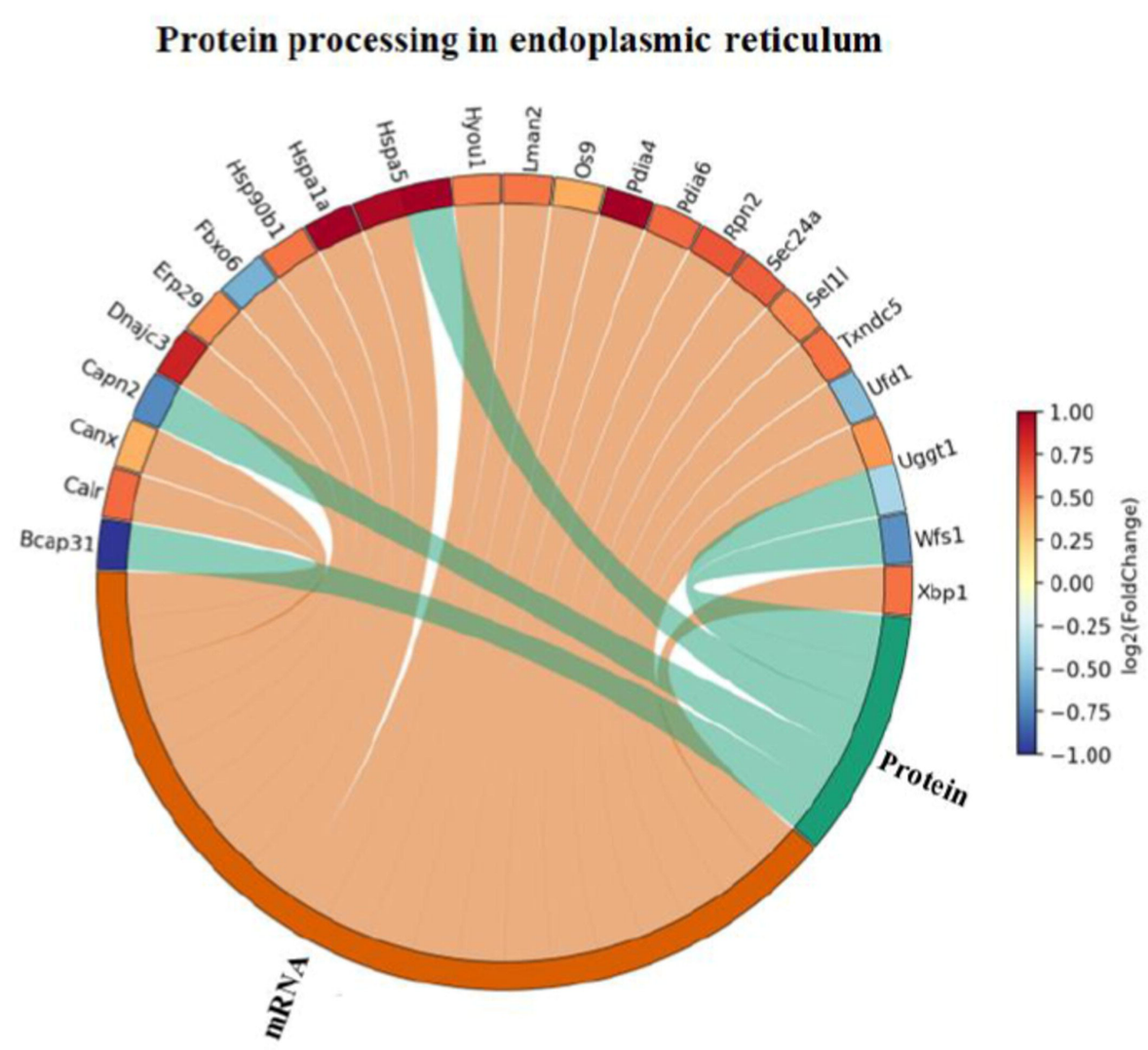
Protein processing in endoplasmic reticulum
Hyou1
Lman2
Os9
Pdia4
Pdia6
Rpn2
Sec24a
Sel1l
Txndc5
Ufd1
Uggt1
Wfs1
Xbp1
Hspa5
Hspa1a
Hsp90b1
Fbxo6
Erp29
Dnajc3
Capn2
Canx
Calr
Bcap31
Protein
mRNA
1.00
0.75
0.50
0.25
0.00
−0.25
−0.50
−0.75
−1.00
log2(FoldChange)

(A)

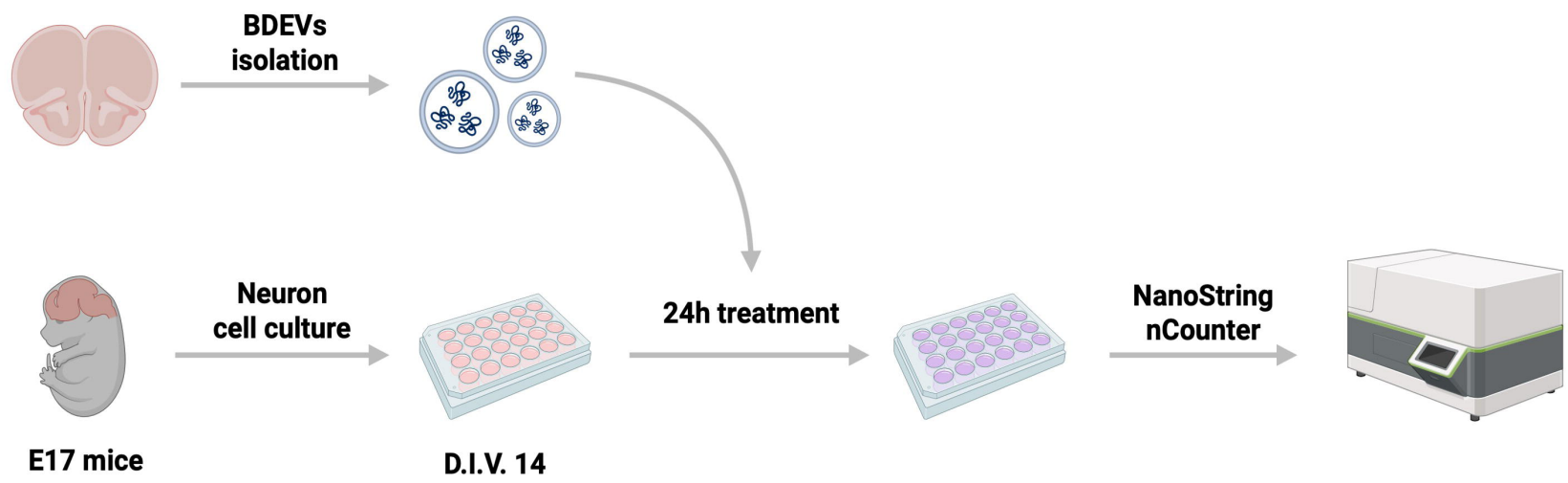
BDEVs
isolation
Neuron
cell culture
24h treatment
NanoString
nCounter
E17 mice
D.I.V. 14

(B)

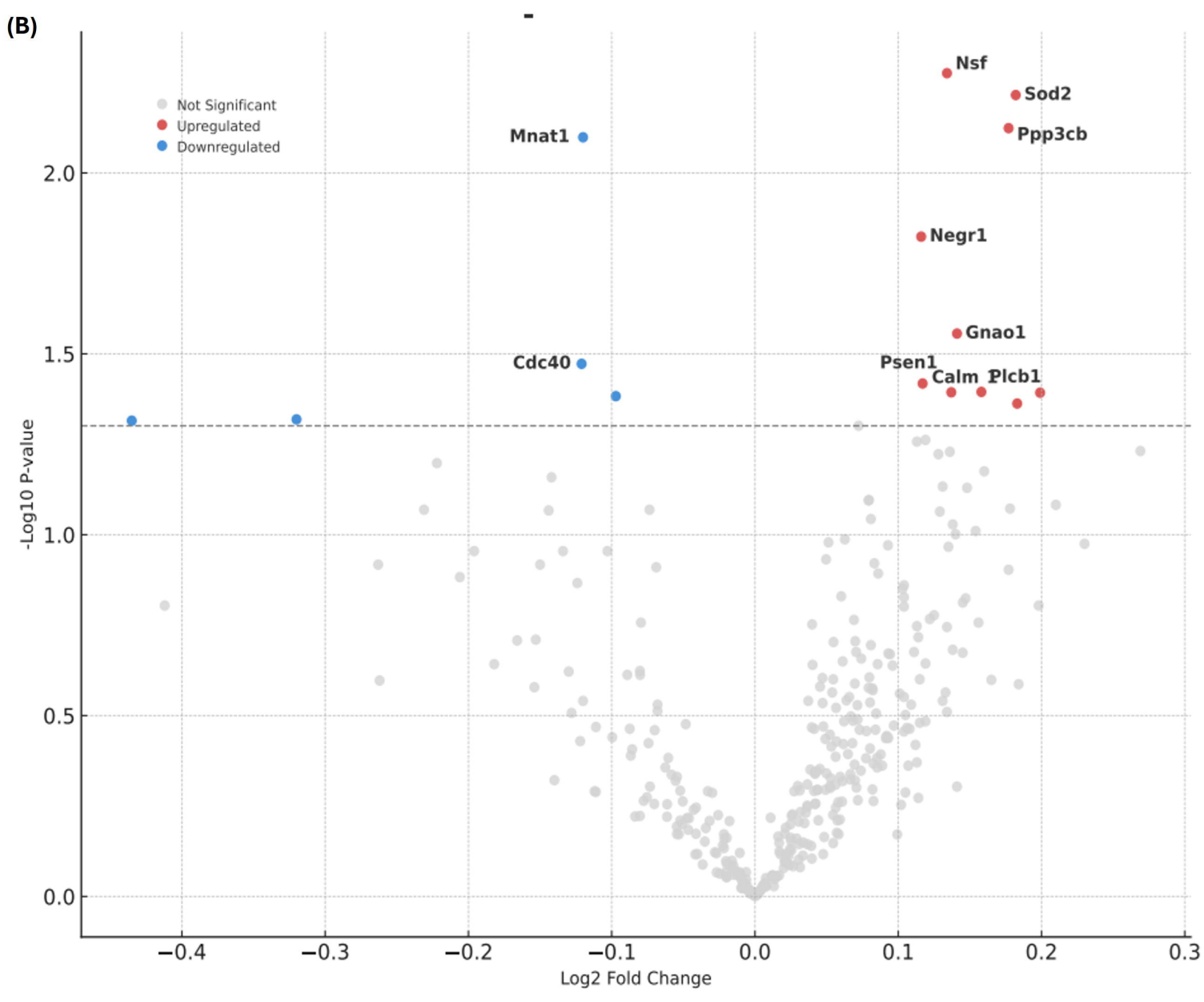
Not Significant
Upregulated
Downregulated
Nsf
Sod2
Ppp3cb
Mnat1
Negr1
Gnao1
Cdc40
Psen1
Calm
Plcb1
-Log10 P-value
Log2 Fold Change
2.0
1.5
1.0
0.5
0.0
−0.4
−0.3
−0.2
−0.1
0.0
0.1
0.2
0.3

(C)

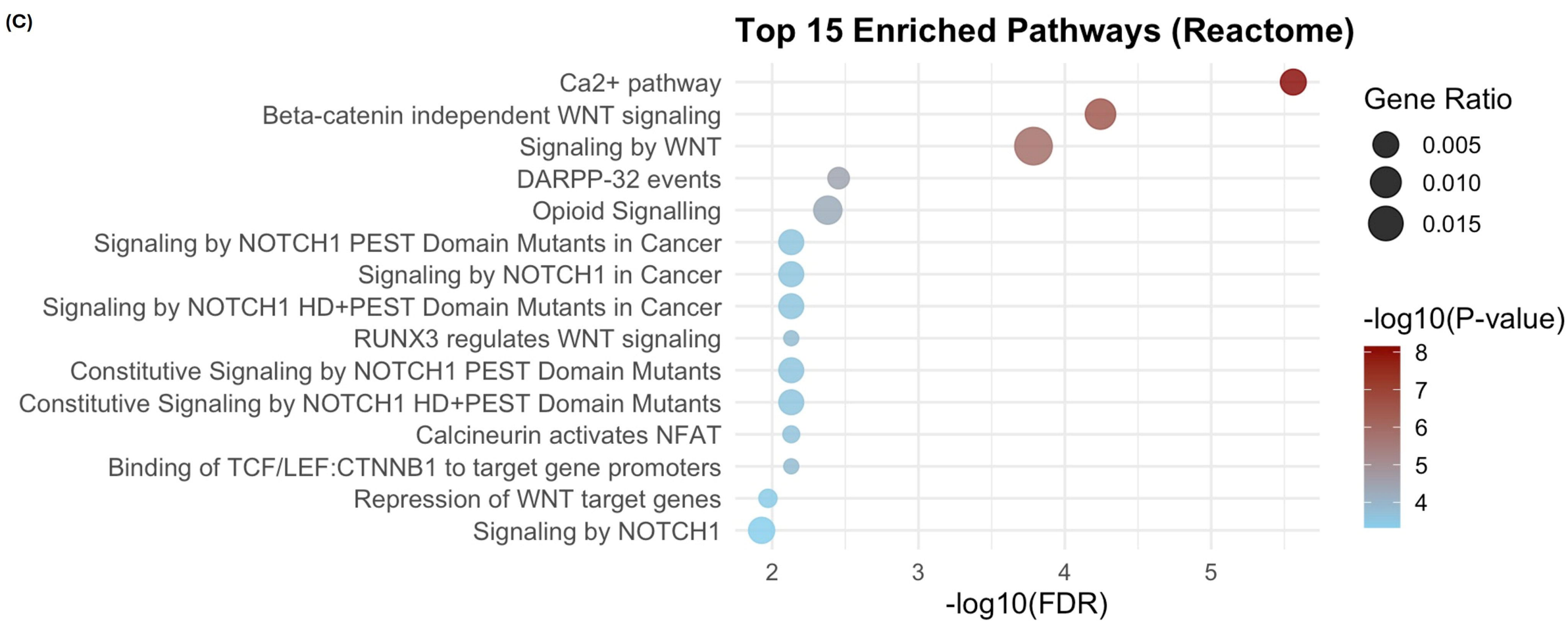
Top 15 Enriched Pathways (Reactome)
Ca2+ pathway
Beta-catenin independent WNT signaling
Signaling by WNT
DARPP-32 events
Opioid Signalling
Signaling by NOTCH1 PEST Domain Mutants in Cancer
Signaling by NOTCH1 in Cancer
Signaling by NOTCH1 HD+PEST Domain Mutants in Cancer
RUNX3 regulates WNT signaling
Constitutive Signaling by NOTCH1 PEST Domain Mutants
Constitutive Signaling by NOTCH1 HD+PEST Domain Mutants
Calcineurin activates NFAT
Binding of TCF/LEF:CTNNB1 to target gene promoters
Repression of WNT target genes
Signaling by NOTCH1
2
3
4
5
-log10(FDR)
Gene Ratio
0.005
0.010
0.015
-log10(P-value)
8
7
6
5
4